One-Step Synthesis of Nano–Micro Chestnut TiO_2 with Rutile Nanopins on the Microanatase Octahedron

Eiji Hosono,[†] Shinobu Fujihara,[‡] Hiroaki Imai,[‡] Itaru Honma,[†] Ichihara Masaki,[§] and Haoshen Zhou[†,*]

[†]National Institute of Advanced Industrial Science and Technology, Umezono, 1-1-1, Tsukuba 305-8568, Japan, [‡]Keio University, 3-14-1, Hiyoshi, Kohoku-ku, Yokohama 223-8522, Japan, and [§]Material Design and Characterization Laboratory, Institute for Solid State Physics University of Tokyo, 5-1-5, Kashiwanoha, Kashiwa, Chiba 277-8581, Japan

ABSTRACT The solution synthesis of large single crystals of octahedron-like anatase TiO_2 is reported, although this novel result is unexpected in the light of reported theoretical calculations. Moreover, systematic control of the crystal growth of rutile nanopins on the microanatase octahedron single crystal results in a nano–micro chestnut-like TiO_2 structure. The control of the formation of rutile nanopins on the large single crystals of anatase in the same solution is an interesting and useful technique, based on thermodynamics and surface chemistry.

KEYWORDS: TiO_2 · anatase · rutile · single crystal · crystal growth

TiO_2 has been investigated for applications in many areas, such as optical materials,[1] superhydrophobic and superhydrophilic materials,[2,3] photocatalytic devices,[4,5] dye-sensitized solar cells,[6] and lithium-ion batteries.[7,8] In particular, many researchers have focused their studies on the control of the nanostructure of TiO_2 for potential applications, because the high surface area resulting from nanostructure control improves the properties of the TiO_2. TiO_2, as a result of its high refractive index, which is higher than that of diamond (rutile TiO_2, 2.76; anatase TiO_2; 2.52; and diamond, 2.42), is also very useful as an optical material for such applications as ultraviolet emitters, lasers, and prisms. To use TiO_2 as an optical material, it is necessary to fabricate single TiO_2 crystals with a controlled crystal phase and morphology. Large single crystals of rutile TiO_2 with a rectangular parallelepiped morphology have been prepared by a solution-based synthesis,[9] but the fabrication of large single crystals of anatase TiO_2 appears to be difficult or impossible, because anatase TiO_2 is a thermodynamically metastable phase and rutile TiO_2 is the more stable phase.[11] Moreover, there are no reports of the fabrication of single-crystalline rutile TiO_2 nanopins on large single-crystalline anatase TiO_2 by a one-step reaction in the same solution. Although many researchers have studied the control of the TiO_2 crystal phase and morphology, it is still difficult to control the fabrication process, particularly to produce a single crystal with an equilibrium shape. The theory of controlling the phase and structure of TiO_2 from the nanoscale to the microscale is a very interesting and important problem from both academic and industrial points of view.

In this work, we report the control of the crystal phase and morphology of single-crystalline TiO_2. A large single-crystalline anatase TiO_2 octahedron at the micrometer scale is first synthesized by a simple solution method. Rutile nanopins with a maximum size of several nanometers can then be fabricated on the anatase octahedron by this simple solution method, forming a nano–micro chestnut-like structure. This control technique will promote a better understanding of the theory of crystal growth, including that of TiO_2 phases, and lead to many new potential applications of TiO_2.

RESULTS AND DISCUSSION

Figure 1 shows scanning electron microscopy (SEM) images of TiO_2 crystals synthesized by hydrothermal treatment of aqueous titanium trichloride ($TiCl_3$; 0.15 mol · dm^{-3}) solutions with sodium dodecyl sulfate (SDS; 0.0133 mol · dm^{-3}). We can see nanopin-like crystals with an octahedral morphology in Figure 1a. The morphology shown in Figure 1b is similar to the chestnut shown in Figure 1d. This nano–micro chestnut-like morphology is observed in the precipitated powder, as shown in Figure 1c. The micrometer-sized octahedral crystals are covered by a nanopin structure. High-magnification views and electron diffraction (ED) patterns recorded by

*Address correspondence to hs.zhou@aist.go.jp.

Received for review May 2, 2007 and accepted October 02, 2007.

Published online October 23, 2007.
10.1021/nn700136n CCC: $37.00

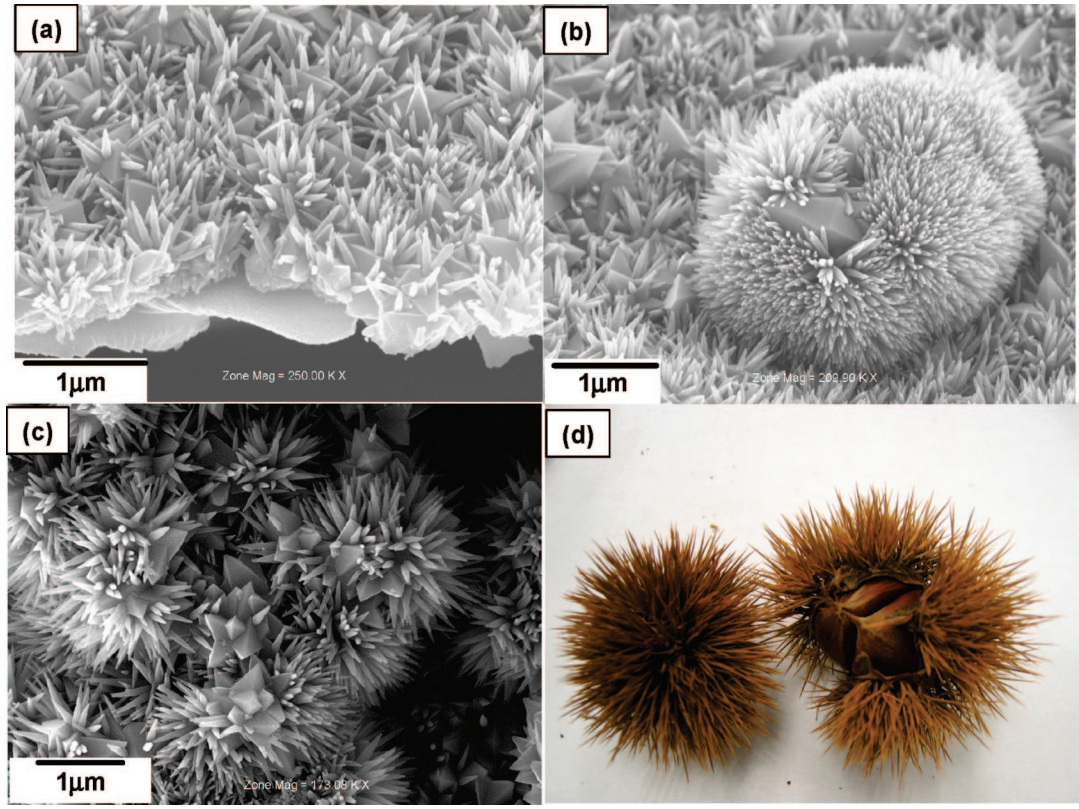

Figure 1. (a,b) SEM images of the film deposited on the substrate at 200 °C, 3 h after treatment of the precursor solution with 0.0133 mol · dm^{-3} SDS: (a) nanopins on the octahedron structure and (b) chestnut-like structure. (c) SEM images of the powder precipitated with 0.0133 mol · dm^{-3} SDS at 200 °C after 3 h. (d) Image of actual chestnuts, with the pin-like integument.

transmission electron microscopy (TEM) are shown in Figure 2. Figure 2a and the ED patterns show that the octahedral morphology and the nanopin structure are single-crystalline anatase-phase TiO_2 and single-crystalline rutile-phase TiO_2, respectively. The top of the rutile pin is a very sharp nanopin with a size of 5 nm, as shown in Figure 2b. Lattice images, which are parallel to the wall, can be clearly seen as a result of phase contrast in the inset image of Figure 2b. The distance between the lattice fringes can be assigned to the interplanar distance of rutile TiO_2 (110), which is $d_{110} = 3.247$ Å. The [110] axis is thus perpendicular to the wall. The nanopin crystals therefore grew along the [001] axis, which is perpendicular to the [110] axis.

We consider that this interesting morphology is a result of the presence of SDS. Figure 3 shows images of TiO_2 crystals synthesized in the absence and in the presence of SDS at concentrations of 0.0133, 0.025, and 0.133 mol · dm^{-3}. When SDS is not present in the precursor solution, rectangular parallelepiped rutile TiO_2 is obtained, as shown in Figure 3a.[9] In the case of low concentrations of SDS, such as 0.0133 and 0.025 mol · dm^{-3}, rutile nanopins grew on the facets of the anatase octahedron, as shown in Figure 3b,c. In the presence of 0.133 mol · dm^{-3} SDS, which is 10 times as much as in the case that led to the formation of the octahedral shape with nanopins shown in Figure 3b, all

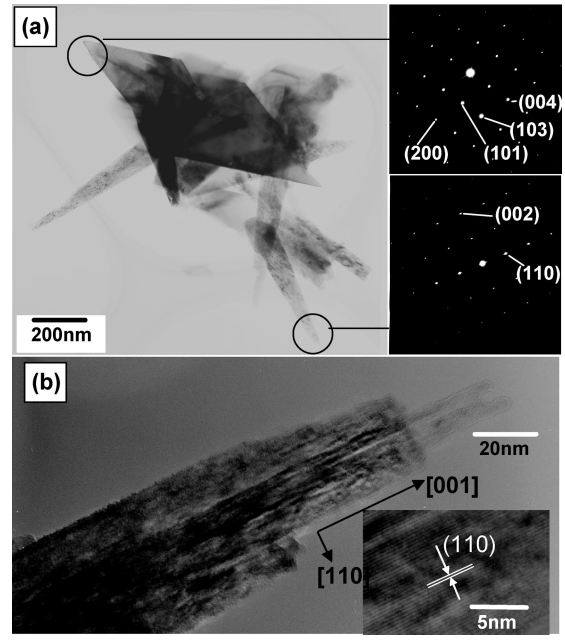

Figure 2. (a) TEM images of the film deposited on the substrate at 200 °C, 3 h after treatment of the precursor solution with 0.0133 mol · dm^{-3} SDS. The ED patterns indicate that the nanopin and octahedral structures are constructed by single-crystalline rutile TiO_2 and single-crystalline anatase TiO_2, respectively. (b) The top of the nanopin structure, with the size of 5 nm. The nanopin grows in the [001] direction.

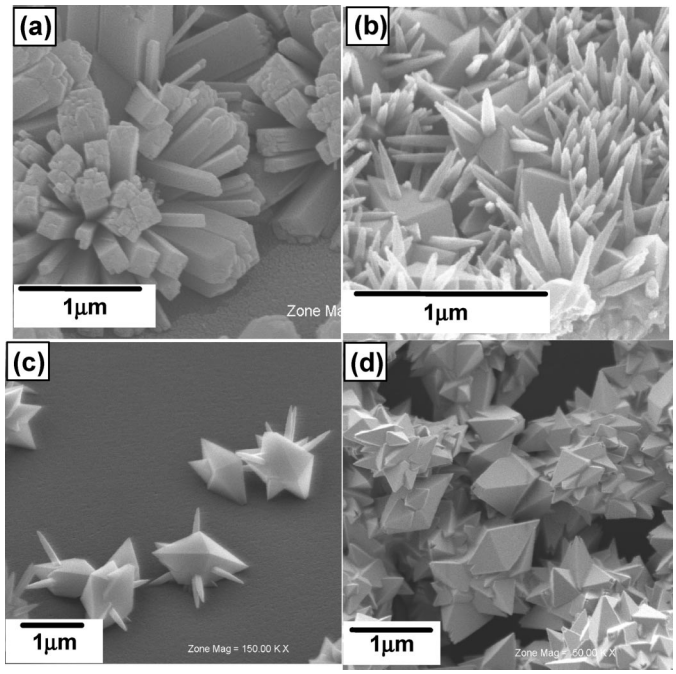

Figure 3. SEM images of the film deposited on the substrate at 200 °C, 3 h after growth of the precursor solution (a) without SDS and after treatment with (b) 0.0133, (c) 0.025, and (d) 0.133 mol · dm^{-3} SDS.

of the crystals appear to have an octahedral morphology, as shown in Figure 3d. Figure 4a is a TEM image of the octahedral crystals in Figure 3d. The distance between the tops of the bipyramids is around 2.5 μm. Figure 4b is a high-resolution TEM of the surface corresponding to the side facet shown in Figure 4a. Lattice images, which are parallel to the facet, can clearly be seen with phase contrast. The distance between the adjacent lattice fringes can be assigned to the interplanar distance of anatase TiO_2 (101), which is $d_{101} = 3.52$ Å. Figure 4c shows an ED pattern of an octahedral crystal.

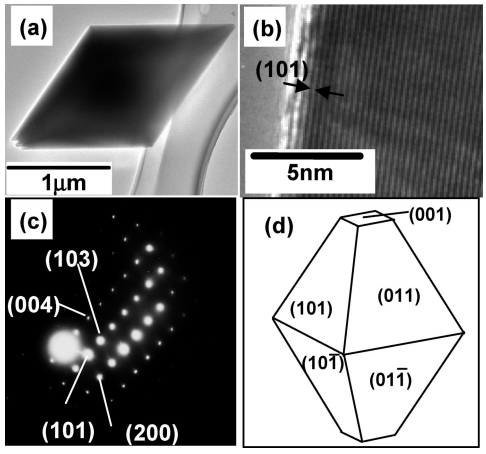

Figure 4. (a) TEM image of one of the anatase TiO_2 octahedrons deposited on the substrate at 200 °C, 3 h after treatment with 0.133 mol · dm^{-3} SDS. The size of the crystal is around 2.5 μm. (b) High-resolution TEM image, showing the lattice of the crystal. (c) ED pattern of the anatase single-crystalline TiO_2 octahedron. (d) Equilibrium shape of anatase TiO_2 according to the Wulff construction and a surface energy calculation.

The spot pattern indicates that the crystal has a single-crystalline nature. We measured the crystallinity by Raman spectroscopy, as shown in Figure 5a for octahedral anatase TiO_2 and in Figure 5b for nanocrystalline anatase TiO_2 (ST-01, Ishihara Sangyo). The octahedral anatase TiO_2 showed a 100 times greater intensity in its Raman spectrum than did nanocrystalline anatase. This shows that the TiO_2 formed has a high crystallinity. If the octahedral particles were constructed from nanosized particles, as in a mesocrystal or oriented architecture,[12–15] the Raman spectrum should be similar to that of ST-01. In this case, however, the Raman spectrum shows very sharp peaks. Moreover, we investigate the particles after milling of the octahedral anatase TiO_2. The fractured parts had sharp edges and were similar to the fractured parts of single-crystalline particles in general (Supporting Information, Figure S1). Thermogravimetry/differential thermal analysis (TG-DTA) of the octahedral anatase TiO_2 particles showed the presence of flat TG curves without any weight loss. This indicates that organic compounds are not present in the TiO_2 particles (Supporting Information, Figure S2). From these results, we can conclude that this crystal consists of single-crystalline anatase TiO_2.

The equilibrium shape of an anatase TiO_2 crystal, according to the Wulff construction and a surface energy calculation,[10] is shown in Figure 4d. Judging from the SEM, TEM, and calculated images, the octahedral anatase TiO_2 crystal has a near-equilibrium shape.

The formation of large anatase crystals, over a micrometer in size, greatly deviates from the theoretical calculations.[11] A recent theoretical report suggests that an anatase phase will transform into a rutile phase when the particle size is larger than several tens of na-

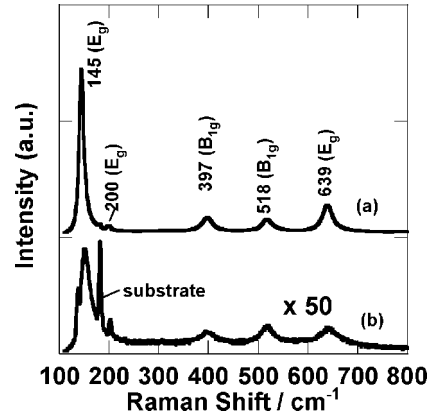

Figure 5. Raman spectra of (a) the large single-crystalline anatase TiO_2 and (b) the nanocrystalline anatase TiO_2 (ST-01, Ishihara Sangyo). The intensity was expanded 50 times.

nometers;[11] in fact, the reported maximum size of anatase TiO_2 is around several tens of nanometers.[16]

The formation of the large single-crystalline anatase TiO_2 and the rutile nanopin on the anatase octahedral TiO_2 occurs by the following mechanism. The most important point is that gradual growth is necessary for the formation of a single-crystal system. Until now, the typical method for synthesizing TiO_2 has involved use of Ti(IV) as a titanium source in conventional sol–gel or solution syntheses. However, the rate of reaction of Ti(IV) in forming TiO_2 is too fast to permit control to allow thermodynamic equilibrium to be attained. Generally, the formation of large single crystals in solution systems is difficult because of the formation of many nuclei as a result of the high degree of supersaturation, which results in the formation of many nanoparticles. When the degree of supersaturation is controlled at a low level, heterogeneous nucleation occurs,[17] homogeneous nucleation decreases, and inorganic materials such as metal oxides are deposited on the substrate. To obtain a low degree of supersaturation, it is therefore necessary to control the reaction rate in the solution. In this study, a slow reaction rate was maintained by using Ti(III) as a titanium source. Ti(III) must first be oxidized to Ti(IV) in order to construct the TiO_2 crystal. This slow oxidation by dissolved oxygen results in the preferential formation of large single crystals with a thermodynamic equilibrium shape.

The second most important point is the use of SDS. Generally speaking, anatase TiO_2 is formed under conditions of relatively high pH, and rutile TiO_2 is formed under conditions of low pH.[18] In the experiment for the production of pure octahedral anatase by using SDS at a concentration of 0.133 mol · dm^{-3}, the pH values of the solution before and after the reaction were 0.91 and 0.44, respectively. Under these pH conditions, the deposition of rutile-phase TiO_2 is possible. Actually, a rutile phase was deposited in the precursor solution (pH 0.94) without SDS. If the pH of the precursor solution is maintained at a high value in order to obtain an anatase phase, the chemical potential of the titanium species is increased. Hence, it is theoretically very difficult to form large single-crystalline anatase TiO_2, because many nanocrystalline nuclei are formed in the solution as a result of the high degree of supersaturation, although an anatase phase is formed. The resultant particles are very small nanoparticles, in the range of several nanometers to several tens of nanometers.

Note, however, that it has been reported that anatase nanoparticles are formed with a crystallite size of 3.5 nm in a solution containing SO_4^{2-}, as a result of the chelating effects of the TiO_6 complex, despite the pH conditions being more suitable for rutile formation.[19] In our work, it is considered that SO_4^{2-} ions were formed by the hydrolysis of SDS into 1-dodecanol and sulfuric acid.[20] In fact, after the reaction, the pH of the solution was decreased, and we could see a hydrophobic liquid floating in the Teflon-lined autoclaves. This liquid was confirmed to be 1-dodecanol by Fourier transform infrared spectroscopy (FT-IR) and X-ray diffraction (XRD) (see Figure 6). The FT-IR spectrum (Figure 6a) of the liquid shows peaks corresponding to C–H (stretching and deformation), O–H (stretching), and S–O (stretching) vibrations. The liquid was solidified by cooling and confirmed to be 1-dodecanol (JCPDS No. 36-1708; mp 23.4 °C) by XRD (Figure 6b). The difference in the peak intensity ratio is caused by orientation, because the solid was formed from the liquid on the glass folder for XRD. The critical energy barrier for heterogeneous nucleation is smallest when the nuclei/substrate interfacial energy is at a minimum. On smooth surfaces, such as glass, the lowest interfacial energy is attained when the lowest-energy planes of the nuclei are aligned parallel to the substrate surface. Judging from the XRD and the S–O vibration, we considered that the liquid consists of 1-dodecanol with SO_4^{2-}.

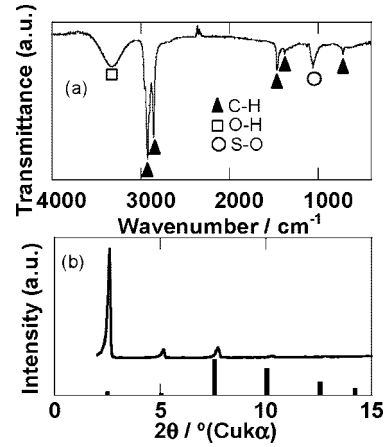

Figure 6. (a) Attenuated total reflectance FT-IR spectrum of the liquid formed after the reaction. (b) XRD pattern of the solid converted from the liquid by cooling.

The FT-IR spectrum of the fabricated octahedral TiO_2 (Supporting Information, Figure S3) confirmed the presence of the sulfate species.[21] The FT-IR spectra were measured by using the KBr method. The peaks show the presence of a sulfate species and of Ti–O bonding. The sulfate species was formed by the hydrolysis of SDS and adsorbed onto the TiO_2.

These results show that the sulfate species derived from SDS caused the formation of the anatase phase. The mechanism for the formation of the anatase single crystal with an equilibrium shape is as follows. First, SO_4^{2-} is formed:

$$C_{12}H_{25}OSO_3^-Na^+ + H_2O \rightarrow C_{12}H_{25}OH + HSO_4^-Na^+$$

$$HSO_4^- + H_2O \rightarrow H_3O^+ + SO_4^{2-}$$

The slow oxidation process from Ti(III) to Ti(IV) occurs *via* dissolved oxygen:[9]

$TiOH^{2+} + O_2 \rightarrow$ Ti(IV) oxo species with $SO_4^{2-} + O^{2-} \rightarrow$ anatase TiO_2 with sulfate species

These reaction processes result in a very low degree of supersaturation, so heterogeneous nucleation and crystal growth occur. The resultant anatase TiO_2 grows into a large single crystal with an octahedral shape. This equilibrium octahedral shape is caused not only by the slow oxidation of Ti(III) to Ti(IV) but also by the decomposition of SDS to give SO_4^{2-}. Large crystals, identified as anatase TiO_2 by XRD, were also obtained when we conducted the experiment in the presence of 0.1 M sulfuric acid instead of SDS. The SEM images (Supporting Information, Figure S4a) show pyramidal shapes: this morphology is similar to that observed in the presence of SDS. However, the TEM image (Supporting Information, Figure S4b) shows slender octahedron-like shapes. A gradual increase in SO_4^{2-} concentration, as achieved by decomposition of SDS, is needed in order to obtain the equilibrium octahedral shapes.

In the theoretical calculation, a thermodynamic model based on surface free energies and surface tensions obtained from first principles affected the morphology and phase stability of TiO_2. However, the model was limited to a surface with only H, OH, and O present.[11] We believe that the presence of other surface chemical species, such as SO_4^{2-}, would change the TiO_2 surface energy and possibly result in the formation of a large-size anatase phase.

The mechanism of the production of the octahedral anatase TiO_2 by SO_4^{2-} derived from SDS explains the formation of the specific morphology, which is rutile TiO_2 nanopins on anatase octahedrons. As shown in Figure 1, the octahedral anatase TiO_2 is formed first on the glass substrate, because the amount of SO_4^{2-} is large in the early stages of the reaction. The formation of anatase TiO_2 consumes the SO_4^{2-} in the solution. In the later stages, the small amount of SO_4^{2-} that is present cannot promote the formation of anatase TiO_2, because the effect of adsorption of SO_4^{2-} decreases, and the thermodynamically favored rutile phase is therefore formed. We consider that the nanopin morphology is the result of the adsorption of small amounts of SO_4^{2-} on rutile TiO_2. The chestnut-like morphology is formed through aggregation of large octahedrons, which can be seen next to the chestnut-like morphology (Supporting Information, Figure S5).

In conclusion, large single-crystalline anatase TiO_2 with an octahedron-like equilibrium morphology was formed. The size of this anatase TiO_2 was much larger than the theoretical limit. The important point in the crystal growth is the control of the chemical reaction in the solution. Slow oxidation of Ti(II) $\rightarrow$ Ti(III) and decomposition of SDS into SO_4^{2-} result in the maintenance of a low degree of supersaturation, which is essential to achieve the conditions necessary for crystal growth. The difference in the concentration of SDS can be easily used to control the crystal phase and morphology, such as a rectangular parallelepiped rutile TiO_2, a chestnut-like morphology with rutile nanopin TiO_2 on the octahedral anatase TiO_2, and octahedral anatase TiO_2. The one-step formation of rutile nanopin on large single-crystalline anatase in the same solution is a result of the progression of the chemical reaction in the solution.

EXPERIMENTAL SECTION

Single-crystal anatase TiO_2 was synthesized by hydrothermal treatment of aqueous titanium trichloride ($TiCl_3$; 0.15 mol · dm^{-3}) solutions with sodium dodecyl sulfate (SDS; 0–0.133 mol · dm^{-3} (Wako Pure Chemicals, Japan). The solution of $TiCl_3$ in dilute aqueous HCl was supplied by Wako Pure Chemicals. The precursor solution (40 mL) was placed in a Teflon-lined autoclave (model 4744, Parr Instrument Co.). Glass slides (S-1111, Matsunami Glass Ind., Ltd., Japan) were used as substrates and were immersed in the solutions. The solutions were then heated at 200 °C for 3 h in a dry oven. The TiO_2 deposited on the substrates was rinsed with deionized water and dried at room temperature.

The crystal structure was examined by X-ray diffraction (XRD) analysis with a Bruker AXS D8 Advance instrument using Cu Kα radiation. The morphology of the film was examined by field-emission scanning electron microscopy (FESEM; Carl Zeiss Gemini Supra) and by high-resolution transmission electron microscopy (HRTEM; JEOL JEM-2010F). Infrared (IR) spectra of the composite materials were recorded by using an FT/IR-6200 IR spectrophotometer (JASCO Corp., Tokyo, Japan). Raman spectra were recorded in the backward geometry on a NIHON BUNKO Ventuno spectrometer (NSR-1000DT) at room temperature. The powder samples were excited by using the 632.8 nm wavelength line from a He–Ne laser.

Supporting Information Available: Figure S1, SEM image of the broken particles after milling of the octahedron anatase TiO_2; Figure S2, TG-DTA curves of the octahedron anatase TiO_2 particles; Figure S3, FT-IR spectrum of the deposited anatase TiO_2; Figure S4, SEM and TEM images of the precipitated anatase TiO_2; and Figure S5, SEM images of the film deposited on the substrate. This material is available free of charge *via* the Internet at http://pubs.acs.org.

REFERENCES AND NOTES

1. Tang, H.; Berger, H.; Schmid, P. E.; Lévy, F. Photoluminescence in TiO_2 Anatase Single Crystals. *Solid State Commun.* **1993**, *87*, 847–850.
2. Wang, R.; Hashimoto, K.; Fujishima, A.; Chikuni, M.; Kojima, E.; Kitamura, A.; Shimohigoshi, M.; Watanabe, T. Light-Induced Amphiphilic Surfaces. *Nature* **1997**, *388*, 431–432.
3. Feng, X.; Zhai, J.; Jiang, L. The Fabrication and Switchable Superhydrophobicity of TiO_2 Nanorod Films. *Angew. Chem., Int. Ed.* **2005**, *44*, 5115–5118.
4. Hoffmann, M. R.; Martin, S. T.; Choi, W.; Bahnemann, D. W. Environmental Applications of Semiconductor Photocatalysis. *Chem. Rev.* **1995**, *95*, 69–96.
5. Fujishima, A.; Honda, K. Electrochemical Photolysis of Water at a Semiconductor Electrode. *Nature* **1972**, *238*, 37–38.

6. Oregan, B.; Grätzel, M. A Low-Cost, High-Efficiency Solar Cell Based on Dye-Sensitized Colloidal TiO_2 Films. *Nature* **1991**, *353*, 737–740.
7. Kavan, L.; Grätzel, M.; Gilbert, S. E.; Klemenz, C.; Scheel, H. J. Electrochemical and Photoelectrochemical Investigation of Single-Crystal Anatase. *J. Am. Chem. Soc.* **1996**, *118*, 6716–6723.
8. Zhou, H. S.; Li, D. L.; Hibino, M.; Honma, I. A Self-Ordered, Crystalline-Glass, Mesoporous Nanocomposite for Use as a Lithium-Based Storage Device with Both High Power and High Energy Densities. *Angew. Chem., Int. Ed.* **2005**, *44*, 797–802.
9. Hosono, E.; Fujihara, S.; Kakiuchi, K.; Imai, H. Growth of Submicrometer-Scale Rectangular Parallelepiped Rutile TiO_2 Films in Aqueous $TiCl_3$ Solutions Under Hydrothermal Conditions. *J. Am. Chem. Soc.* **2004**, *126*, 7790–7791.
10. Lazzeri, M.; Vittadini, A.; Selloni, A. Structure and Energetics of Stoichiometric TiO_2 Anatase Surfaces. *Phys. Rev. B* **2001**, *63*, 155409/1–9.
11. Barnard, A. S.; Curtiss, L. A. Prediction of TiO_2 Nanoparticle Phase and Shape Transitions Controlled by Surface Chemistry. *Nano Lett.* **2005**, *5*, 1261–1266.
12. Oaki, Y.; Imai, H. Nanoengineering in Echinoderms: The Emergence of Morphology from Nanobricks. *Small* **2006**, *2*, 66–70.
13. Oaki, Y.; Kotachi, A.; Miura, T.; Imai, H. Bridged Nanocrystals in Biominerals and their Biomimetics: Classical Yet Modern Crystal Growth on the Nanoscale. *Adv. Funct. Mater.* **2006**, *16*, 1633–1639.
14. Niederberger, M.; Cölfen, H. Oriented Attachment and Mesocrystals: Non-Classical Crystallization Mechanisms Based on Nanoparticle Assembly. *Phys. Chem. Chem. Phys.* **2006**, *8*, 3271–3287.
15. Cölfen, H.; Antonietti, M. Mesocrystals: Inorganic Superstructures Made by Highly Parallel Crystallization and Controlled Alignment. *Angew. Chem., Int. Ed.* **2005**, *44*, 5576–5591.
16. Penn, R. L.; Banfield, J. F. Morphology Development and Crystal Growth in Nanocrystalline Aggregates Under Hydrothermal Conditions: Insights from Titania. *Geochim. Cosmochim. Acta* **1999**, *63*, 1549–1557.
17. Bunker, B. C.; Rieke, P. C.; Tarasevich, B. J.; Campbell, A. A.; Fryxell, G. E.; Graff, G. L.; Song, L.; Liu, J.; Virden, W.; McVay, G. L. Ceramic Thin-Film Formation on Functionalized Interfaces Through Biomimetic Processing. *Science* **1994**, *264*, 48–55.
18. Yamabi, S.; Imai, H. Crystal Phase Control for Titanium Dioxide Films by Direct Deposition in Aqueous Solutions. *Chem. Mater.* **2002**, *14*, 609–614.
19. Li, Y.; Lee, N. H.; Hwang, D. S.; Song, J. S.; Lee, E. G.; Kim, S. J. Synthesis and Characterization of Nano Titania Powder with High Photoactivity for Gas-Phase Photo-oxidation of Benzene from $TiOCl_2$ Aqueous Solution at Low Temperatures. *Langmuir* **2004**, *20*, 10838–10844.
20. Bethell, D.; Fessey, R. E.; Namwindwa, E.; Roberts, D. W. The Hydrolysis of C-12 Primary Alkyl Sulfates in Concentrated Aqueous Solutions. Part 1. General Features, Kinetic Form and Mode of Catalysis in Sodium Dodecyl Sulfate Hydrolysis. *J. Chem. Soc., Perkin Trans. 2* **2001**, 1489–1495.
21. Yang, Q. J.; Xie, C.; Xu, Z.; Gao, Z.; Du, Y. Synthesis of Highly Active Sulfate-Promoted Rutile Titania Nanoparticles with a Response to Visible Light. *J. Phys. Chem. B* **2005**, *109*, 5554–5560.